A Portable Vision-Based Real-Time Lane Departure Warning System: Day and Night

Article *in* IEEE Transactions on Vehicular Technology · June 2009

DOI: 10.1109/TVT.2008.2006618 · Source: IEEE Xplore

4 authors, including:

Pei-Yung Hsiao
National University of Kaohsiung
129 PUBLICATIONS **933** CITATIONS

SEE PROFILE

Shih-Shinh Huang
National Kaohsiung First University of Science and Technology
43 PUBLICATIONS **563** CITATIONS

SEE PROFILE

Li-Chen Fu
National Taiwan University
582 PUBLICATIONS **5,996** CITATIONS

SEE PROFILE

A Portable Vision-Based Real-Time Lane Departure Warning System: Day and Night

Pei-Yung Hsiao, Chun-Wei Yeh, Shih-Shinh Huang, and Li-Chen Fu

***Abstract*—Lane departure warning systems (LDWS) are an important element in improving driving safety. In this paper, we propose an embedded Advanced RISC Machines (ARM)-based real-time LDWS. As for software development, an improved lane detection algorithm based on peak finding for feature extraction is used to successfully detect lane boundaries. Then, a spatiotemporal mechanism using the detected lane boundaries is designed to generate appropriate warning signals. As for hardware implementation, a 1-D Gaussian smoother and a global edge detector are adopted to reduce noise effects in the images. By using the developed data transfer channel (DTC) in the reconfigurable field-programmable gate array (FPGA) module, the data transfer rate among the complementary metal–oxide–semiconductor (CMOS) imager module, liquid-crystal display (LCD) display module, and central processing unit (CPU) bus is about 25 frame/s for an image size of 256 × 256. In addition, the proposed departure warning algorithm based on spatial and temporal mechanisms is successfully executed on the presented ARM-based platform. The effectiveness of our system concludes that the lane detection rate is 99.57% during the day and 98.88% at night in a highway environment. The proposed departure mechanisms effectively generate effective warning signals and avoid most false warnings.**

***Index Terms*—Computer vision, embedded real-time system, lane departure warning system (LDWS), lane detection, smart vehicle, vanishing point.**

I. Introduction

Traffic accidents have become one of the most serious problems today, and most of them occur due to driver negligence. Therefore, many works have been done to investigate ways of developing a driving-assistance system to improve driving safety. Currently, many proposed systems are still implemented on personal computer (PC)-based platforms, which means they lack flexibility for easy deployment and capability of product commercialization. Hence, the main objective of this paper is the development of a portable real-time lane departure warning system (LDWS) with properties including low cost, easy installation, and high compatibility. Fig. 1 shows the concept of our proposed portable device. In achieving this, two issues are addressed here: One is to develop a lane departure warning algorithm based on a robust lane detection method, and the other one is to design a well-suited portable platform to perform the proposed algorithm.

In previous LDWS research studies, as we have known, there was no realization on an embedded portable platform. Most of this research has developed algorithms on a PC-based platform. However, due to the enhancement of embedded calculating technology, much research has already started to exploit the low-cost and high-flexibility advantages of embedded system technology in various other fields. Segura-Jurez *et al.* [1] used a proposed portable electrocardiograph recorder in biomedical engineering. Perera *et al.* [2] proposed their portable electronic nose ipNose in the electronic sensor field. The embedded face-recognition system proposed in [3] can bring high processing efficiency and low cost.

Fig. 1. Concept of a portable real-time LDWS.

Unfortunately, there is a lack of exact discussion on LDWSs exploring the advantages of embedded system technologies. Although a few lane-detection-related papers discussed the possibility of building an algorithm on embedded platforms [4], most papers of this kind neither describe too many details on their hardware sections nor utilize their own customized platforms. In this paper, we are going to present our customized embedded platform, including hardware and software. We believe that if LDWS can be built into portable devices, driving safety will substantially be enhanced. Furthermore, most vehicles, which are not limited to the latest cars or concept vehicles, can use such a device to enhance driving safety.

Although lane departure warning mechanisms have been discussed in the literature, most of the aforementioned papers pay more attention to the lane detection part, without specifically evaluating their warning mechanisms in different situations. In this paper, we not only present our lane detection results but also evaluate our system with a wide variety of vehicle departure situations in daytime and nighttime, as well as discuss the detailed results of the lane departure warning mechanism.

In the lane departure warning part, several researches utilized the angle-based lane departure warning algorithm. Jung and Kelber [5] proposed an algorithm based on the linear–parabolic model, where the image is separated into two vision fields: 1) near, which uses a linear function, and 2) far, which uses a parabolic function. It then uses the corresponding orientations to the lane departure warning method after determining the left and right linear functions of the lane boundaries. Lee *et al.* [6] proposed a lane departure warning algorithm based on the ratio of the lane angles and the distances of two lane boundaries. Hsu *et al.* [7] proposed a kind of lane departure warning algorithm that is based on angle variation. However, the angle-based lane departure warning algorithm will cause too many false negatives due to the very obvious variation of angles in most situations. As a result, some researches started to focus on some other lane departure features, such as lateral offset. Jung and Kelber have tried to use their lane departure warning algorithm in [8], using lateral offset. Kibbel *et al.* [9] also used the lateral position and the lateral velocity based on road-marking detection for lane departure detection. Nevertheless, to obtain the lateral offset from the frames, some further calculations are needed. Most of these LDWSs only adopt a kind of warning mechanism and may cause some false positives and negatives in some situations. For instance, the lane-angle-based algorithm may cause some false

Manuscript received July 17, 2007; revised January 16, 2008 and June 2, 2008. First published October 3, 2008; current version published April 22, 2009. This work was supported by the National Science Council of the Republic of China under Grant NSC96-2516-S390-001-MY3.

P.-Y. Hsiao is with the Department of Electrical Engineering, National Kaohsiung University, Kaohsiung 811, Taiwan (e-mail: pyhsiao@nuk.edu.tw).

C.-W. Yeh is with the Department of Electronic Engineering, Chang Gung University, Tao-Yuan 333, Taiwan (e-mail: chunwei.yeh@gmail.com).

S.-S. Huang is with the Department of Computer and Communication Engineering, National Kaohsiung First University of Science and Technology, Kaohsiung 811, Taiwan (e-mail: powwhuang@gmail.com).

L.-C. Fu is with the Department of Computer Science and Information Engineering, National Taiwan University, Taipei 106, Taiwan (e-mail: lichen@ntu.edu.tw).

Color versions of one or more of the figures in this paper are available online at http://ieeexplore.ieee.org.

Digital Object Identifier 10.1109/TVT.2008.2006618

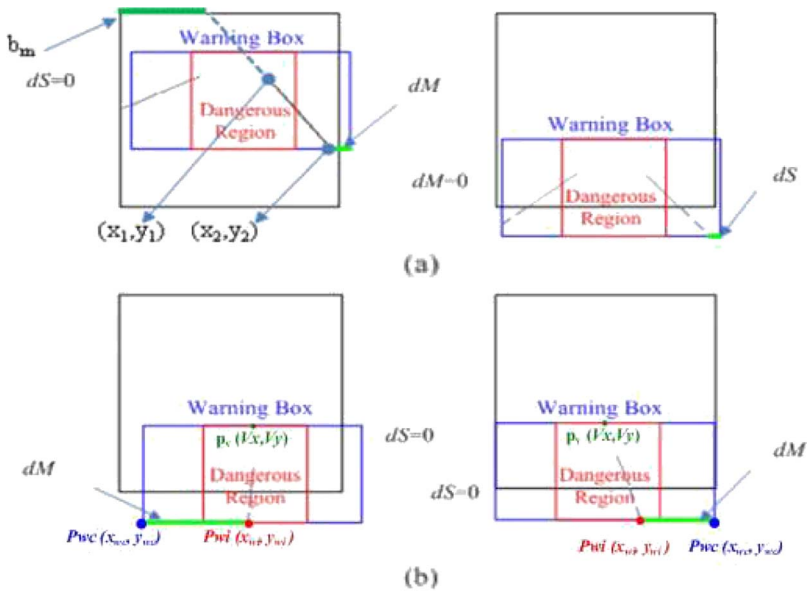

Fig. 2. Warning box and dangerous region in different cases. (a) No warning. (b) Warning.

positives when the vehicle is along one side of the lane channel, instead of departing from it. We believe that too many false positives may cause drivers' nervousness, and too many false negatives may bring crucial danger.

As a result, we use a dual-mechanism warning algorithm to avoid false alarms. The first warning mechanism only focuses on the position of lane boundary intercepts, which can directly be obtained from the image with no complex calculation. The warning signal will be triggered only when the lane boundary intercept is very close to the central part of image, which means that the vehicle is between two lane channels. Furthermore, to predict some lane departure situations and avoid the false positives of the a-little-close-to-one-side situation—not the crossing or departure–we therefore proposed another warning mechanism based on the lane intercept changing rates. Since the dual mechanisms independently worked, their drawbacks will be covered by the other mechanism, and the possibility of false alarm will be reduced to the least extent. Here, our experiments focused on various conditions in daytime and nighttime but are not characterized in a sharp tortuous path or other nonflat road.

The remainder of this paper is organized as follows: In Section II, we will describe our system operating flow and our algorithm and map each procedure to hardware and software operation. In Section III, we will present each module of our hardware system, including the functions implemented using the reconfigurable module. In Section IV, the system prototype will be presented, and we used six video clips with various vehicle departure situations to evaluate our warning system by monitoring the lane detection results, warning signals, and the trend of variables used to judge the departure situation. Conclusions and future work are then given in Section V.

II. Lane Departure Warning Algorithm Using Spatial and Temporal Mechanisms

To improve our previous work [10], a lane departure warning algorithm consisting of two parts, i.e., lane detection and lane departure detection, was proposed in this paper.

A. Lane Detection

The purpose of the lane detection is to find the lane boundaries given by the currently observed image. To filter out noise effect, we first apply a 1-D Gaussian smoothing filter to the input image. Then, a modified algorithm based on the global edge detector proposed in [11] is adopted to successfully detect the lane marks. The global edge detector is based on the difference among the pixels in a 3×3 mask. For easy implementation, the equations for computing the mean $\mu_{x,y}$ and standard deviation $\sigma_{x,y}$ in [12] are modified to

$$\mu_{x,y} = \left(\frac{1}{8} - \frac{1}{64}\right) \sum_{\Delta x=-1,\Delta y=-1}^{\Delta x=+1,\Delta y=+1} g(x+\Delta x, y+\Delta y)$$

$$\sigma_{x,y} = \left(\frac{1}{8} - \frac{1}{64}\right) \sum_{\Delta x=-1,\Delta y=-1}^{\Delta x=+1,\Delta y=+1} |g(x+\Delta x, y+\Delta y) - \mu_{x,y}| \,. \quad (1)$$

According to the obtained edge map, the method related to our previous work [13] is used to detect the lane boundaries. The lane boundary in our detected lane candidates that passes through the most numbers of peak points is called the master lane. The slave lane candidates are defined as the detected lane candidates with the opposite slope of the master lane that pass through the most numbers of peak points. Let $M(a_m, b_m)$ and $S(a_s, b_s)$ be the obtained master and slave lane boundaries, respectively. Here, a_m is the slope of the master lane, and b_m is the intercept of the master lane. Accordingly, a_s and b_s are similar variables for the slave lane. The schematic is shown in Fig. 2. The detected $M(a_m, b_m)$ and $S(a_s, b_s)$ are used to achieve lane departure detection, as described in the next section.

B. Lane Departure Detection Based on Spatial and Temporal Mechanisms

In general, the dangerous lane departure situations result from the following two cases: 1) The driver gets too close toward the lane boundaries. 2) The host vehicle keeps a rapid departure speed, i.e., the host vehicle approaches the lane boundaries too fast. Therefore, we propose the spatial and temporal mechanisms to detect these two departure situations, respectively.

Prior to detailing the warning mechanism, we introduce how to detect the vanishing point. The vanishing point is a point in the image plane to which a set of parallel lines in the 3-D space will converge. Similar to the idea in [14], we use the vanishing point to automatically determine a warning box for lane departure warning and identify the

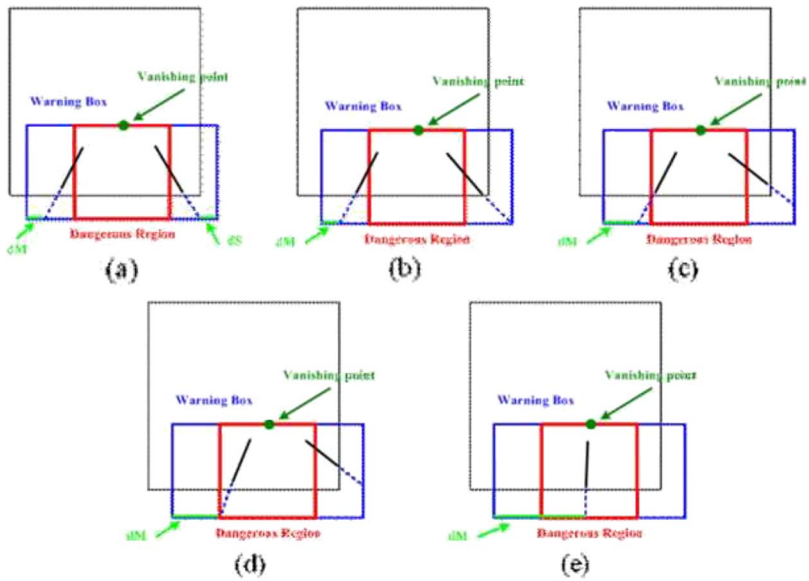

Fig. 3. Changes in d_M and d_S while the host vehicle is moving toward its left lane boundary.

region of interest to save processing time. To overcome the vehicle vibration and image noise suffered in [15], we find 50 vanishing points from the first 50 frames, respectively, and then use the statistical method to compute vanishing point $p_v = (v_x, v_y)$.

1) Spatial Mechanism: The spatial mechanism is designed to identify whether the vehicle is on the verge of dangerous road positions. First, we define the *Warning Box* as a rectangle whose width is equal to the image width and height is half of the image height. Then, the half point of the top boundary of the warning box is positioned at the vanishing point $p_v = (v_x, v_y)$ previously obtained. The *Dangerous Region* is defined as the region centered at the warning box whose width is half that of the image, as shown in Fig. 2. In addition, Fig. 2 shows the warning box in blue and the dangerous region in red.

Suppose that d_M and d_S are the distances from the intercept points $M(a_m, b_m)$ and $S(a_s, b_s)$, respectively, to the near bottom corners of the warning box. From Fig. 2(b), the red intersection $P_{wi}(x_{wi}, y_{wi})$ is the cross point between the extension of the master lane and the base line of the warning box. The blue corner $P_{wc}(x_{wc}, y_{wc})$ is the bottom corner point of the warning box. d_M is defined as the distance between P_{wi} and P_{wc}. Similarly, we can define d_S for the slave lane. When the red intersections P_{wi} are located outside the warning box, both d_M and d_S are set to zero. Consequently, the derivations of d_M and d_S can be expressed as follows:

$$\begin{cases} d_M = \frac{\left(v_y + \frac{1}{2}I_h\right) - b_m}{a_m} - \left(v_x - \frac{1}{2}I_w\right) \\ d_S = \left(v_x + \frac{1}{2}I_w\right) - \frac{\left(v_y + \frac{1}{2}I_h\right) - b_s}{a_s}, \quad \text{if } a_m > 0 \end{cases}$$
$$\begin{cases} d_M = \left(v_x + \frac{1}{2}I_w\right) - \frac{\left(v_y + \frac{1}{2}I_h\right) - b_m}{a_m} \\ d_S = \frac{\left(v_y + \frac{1}{2}I_h\right) - b_s}{a_s} - \left(v_x - \frac{1}{2}I_w\right), \quad \text{otherwise.} \end{cases} \tag{2}$$

The spatial warning mechanism starts to alarm if either d_M or d_S is larger than $1/4I_w$, where I_w and I_h in (2) are the image width and height, respectively.

2) Temporal Mechanism: In addition to spatial mechanism, a warning mechanism based on temporal information is proposed here to detect the dangerous situation in which the host vehicle approaches the lane boundaries too fast. The idea behind temporal mechanism is to verify whether the large value change in d_M and d_S occurs. Let $l(t)$ be the average of the sum of d_M and d_S over frames starting from time t and back to time $t - n$. The definition of $l(t)$ can be expressed as follows:

$$l(t) = \frac{\sum_{i=1}^{n} \left(d_M(t-i) + d_S(t-i)\right)}{\Delta t} \tag{3}$$

where n is the number of frames used to compute $l(t)$. Variable ζ defined as

$$\zeta = l(t_1) - l(t_2) \tag{4}$$

presents the difference between two different time instants t_1 and t_2.

Consider the lane change of the host vehicle to its left side boundary, as shown in Fig. 3. To choose a proper time interval between t_1 and t_2, the detailed variations of d_M and d_S need to be analyzed accordingly in a consecutive manner based on the illustrations in Fig. 3(b)–(e). In the beginning stage, the host vehicle starts to move closely toward its left lane boundary, as shown in Fig. 3(a) and (b). The value of d_S becomes zero, and d_M increases during the interval from Fig. 3(a) and (b), whereas both d_M and d_S were positive in the stage shown in Fig. 3(a). Then, d_M continues to increase, as shown in Fig. 3(b)–(e). Overall, we have observed that the lane change of the host vehicle may cause the sum of d_M and d_S to increase during the stages shown in Fig. 3(b)–(e). The heuristic rules that we adopted are to calculate ζ every nine frames, i.e., $n = 9$. The images captured from the camera have a rate of 25 frame/s in our experiments. As a result, the $l(t)$ in our proposed temporal warning mechanism is updated every 0.36 s. The time interval relation between t_1 and t_2 is then defined as $t_1 + 0.36 = t_2$.

The temporal warning mechanism is designed as follows: If ζ is larger than a threshold value of T_l, i.e., $\zeta > T_l$, then the system will buzz a warning sound. In this situation, the vehicle very quickly changes to another lane channel. From (2), the system is triggered to alarm when the vehicle is close to the lane boundary within a threshold distance that is based on the spatial warning mechanism. However, if the vehicle is still outside of the threshold distance but is going fast and very quickly moving close toward the lane boundary, the driver would not have enough time to turn back and prevent the vehicle from touching and crossing the lane boundary. In this case, the alarm triggered by the spatial warning mechanism will be too late to guarantee the safety of the driving. Therefore, the temporal warning mechanism was proposed to provide urgent warning before the spatial

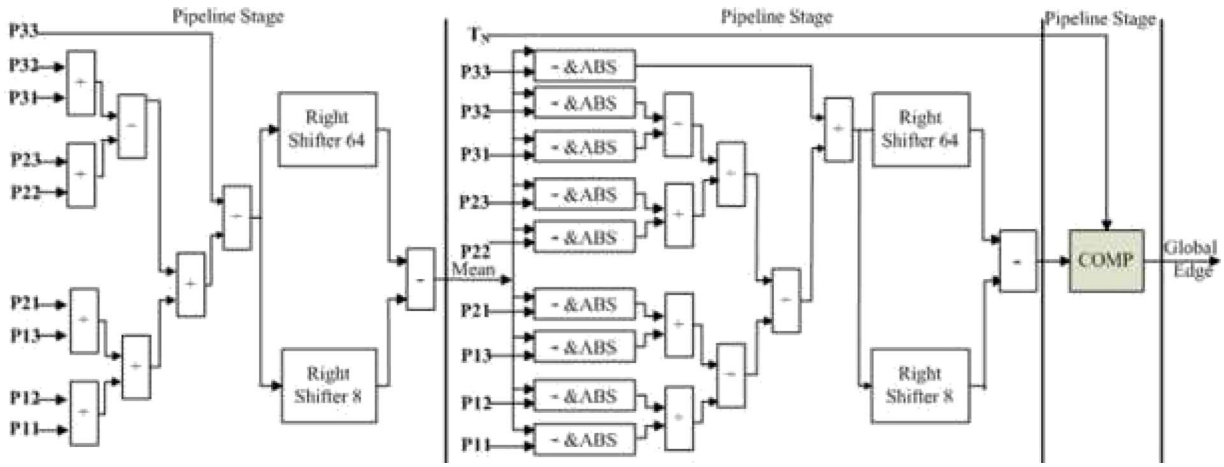

Fig. 4. Architecture of the global edge detector.

warning mechanism triggers the normal alarm. Based on (3), (4), and the aforementioned heuristics shown in Fig. 3(a)–(e), if the values of ζ, which are updated every 0.36 s, are larger than the threshold, the alarm is triggered by the temporal warning mechanism accordingly to avoid possible abrupt collisions.

III. Architecture of LDWS

To make our lane departure warning algorithm a real-time portable device for easy deployment and to charge less in device expenses, a hardware architecture combining ARM7 with a field-programmable gate array (FPGA) to implement our algorithm has been proposed in this paper. In general, our system consists of two parts: 1) the system core and 2) the peripherals.

A. Core Architecture

The system core is composed of two modules: 1) the embedded processor module and 2) the reconfigurable FPGA module. The embedded process module executes all the processes of LDWS, and the reconfigurable FPGA module is responsible for image preprocessing and image transfer among different modules. Since ARM processors are characterized by their low cost, low power consumption, and high performance, they are widely used in embedded systems. The embedded memory controller provides an external memory bus interface that supports various memory chips in different operating modes. Consequently, we adopt the ARM-based processor for designing our system. Furthermore, to optimize memory utilization, some parameters can recursively be accumulated and restored in the memory buffers, instead of preserving a block of memory to store each of them in every interval. For example, considering (3), $l(t)$ can be obtained from d_M, d_S, and Δt, where both d_M and d_S were calculated using (2). The time interval of Δt is constant. We first calculate and keep the average of d_M and d_S in a memory buffer. The values in this buffer can be updated every iterative generation of the new average of d_M and d_S. This way, an efficient memory utilization scheme in embedded systems has been obtained.

The purpose of the FPGA device in our system is to connect the memory bus with the image sensor and the liquid-crystal display (LCD) module. Therefore, testability and extendibility can easily be achieved. In addition, some fundamental image processing units, such as the Gaussian smoothing filter and the global edge detector, are implemented on the FPGA to cooperate with the ARM processor for speeding up the computation time.

Fig. 4 shows our architecture implementation of the global edge detector on the FPGA. However, the transmission speed is a challenging task for a real-time system. Therefore, to speed up the transmission throughput for the real-time requirement, we develop a data transfer channel scheme. This makes the interconnection inside the FPGA successfully use the system memory bus, instead of the general-purpose input/output (GPIO). Using the memory controller and the AMBA high-performance bus to communicate with the ARM core, we obtain a speed up of two times rather than when using the GPIO and the advanced peripheral bus.

B. Peripherals

In addition to the core architecture, some peripherals are constructed to complete the architectural scheme of the embedded platform.

1) Input/Output Module: The input devices of a portable LDWS are the image sensor, which extracts the images, and the keypad, which controls the signals. The main output devices are the LCD module, which displays the results after image processing, and the buzzer, which produces the warning sounds.

2) Storage Module: In our prototype, we use the 2-MB flash read-only memory to store the machine code of our proposed programs. The 16-MB synchronous dynamic random access memory is the main memory of our embedded system.

3) Power Supply Module: Power consumption has a significant impact on system cost and reliability. We utilized low-power-consumption devices and a high-efficiency regulator to build a better power supply module.

IV. Experiment

A hardware platform with an embedded warning system is implemented. The core processor is an ARM7 32-bit reduced-instruction-set-computer central processing unit (CPU) with 66 MHz, and the field-programmable device is an FPGA that has 138 000 logic cells. The power consumption of our platform is about 1 W, and the processing performance for an image size of 256 $\times$ 256 is about 25 frame/s after the camera-calibration procedure. In our experiments, three clips captured at daytime in a highway environment, as well as three clips captured at nighttime, are used. The results of an example of lane detection processed step by step are shown in Fig. 5. Each step in Fig. 5 is meaningful and necessary for the whole algorithm. For example, the step from Fig. 5(d) to Fig. 5(e) clusters the peak points into groups. Some parse and discrete points are ignored during the processing. Then, all the grouped points are shown in Fig. 5(e). For every group, the step from Fig. 5(e) to Fig. 5(f) converts and approximates one group into a line segment. Fig. 5(f) stores the parameters corresponding to the points that can recover and construct all the line segments.

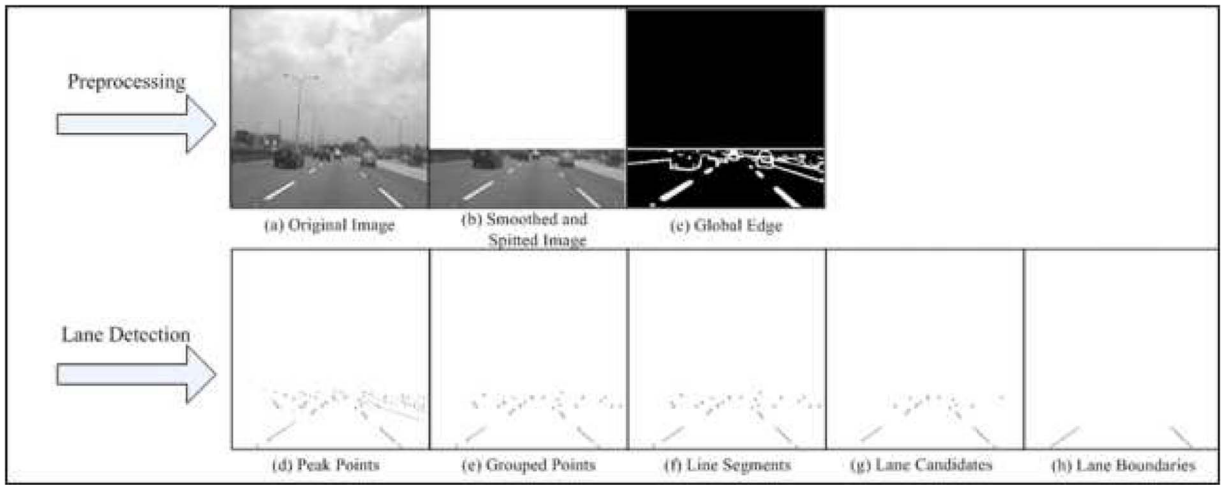

Fig. 5. Results for lane detection processed step by step, with $(v_x, v_y) = (150, 180)$ and $T_N = 8$ in the road image with a resolution of 256 × 256.

TABLE I
FRAME-BASED SUCCESSFUL DETECTION RATE AND FALSE WARNING RATE

Day / Night	Clips	Frames	Hit	Miss	Micro hit rate
	Normal	887	887	0	100.00%
Day	Lane Changing	1117	1111	6	99.46%
	Approaching	1020	1013	7	99.31%
	Total	3024	3011	13	99.57%
	Slowly Move	575	572	3	99.47%
Night	No-Street-Light	1317	1291	26	98.03%
	Perfect in Night	1154	1151	3	99.74%
	Total	3046	3012	32	98.88%
Day & Night	Total	6070	6025	45	99.25%

This step does not consume much computation time, because the number of points is much less than the total number of pixels in an image.

For the parameters in the temporal warning mechanism, we set the interval of $\zeta = [+0.2, -0.2]$ and $T_l = 0.2$. The interval values of ζ and the T_l value were obtained by empirical analysis. The average detection rate of lane detection can be more than 99% under different traffic situations and lighting conditions. Table I shows the statistics of the detection rate over the six clips previously described. In the succeeding sections, we will elaborate on the experimental results of the lane detection and lane departure detection of these six clips.

A. Frame-Based Daytime Evaluation

In the first clip referred in the normal condition, the lane marks are well painted, and no unfavorable phenomena are presented. Therefore, lane detection can be achieved up to 100%. Accordingly, the warning signals are also correctly triggered. The spatial warning mechanism is triggered when $M(a_m, b_m)$ and $S(a_s, b_s)$ are more than 86, which is the warning box border defined by the vanishing point. The system started to warn at the 202nd frame and stopped at the 240th frame. No false warning is triggered in this clip. The temporal warning is triggered at the 200th frame, which happens earlier than the spatial warning. In addition, it is interesting that we also detected the temporal warning at the 460th frame, because the vehicle ran over an obstacle, which ended up in possible departure.

The second clip exhibits the changing-lane situation. The warning box border defined by the vanishing point is 85. The spatial warnings start at the 493rd and 827th frames, and the temporal warnings are triggered at the 460th and 820th frames. The approaching situation, which means that the host vehicle is approaching the vehicle in front, is demonstrated in clip three. Unfortunately, when the vehicle starts to cross the lane, the distance between it and the car in front on the same lane is too short, thus resulting in false lane detection. The unsatisfactory detection results from the case where lane boundaries are occluded by the front vehicle. This problem can be solved by incorporating the information from the vehicle detection.

As a result, lane detection fails in several frames and causes false negatives when it departs from the center of the lane. The system starts to warn at the 895th frame and stops at the 943rd frame. We also detect the temporal warning at the 270th frame since the host vehicle moves close toward the lane boundary at fast speed (see Table II).

B. Frame-Based Nighttime Evaluation

The first nighttime clip shows that the vehicle has slow motions. Although the system fails to trigger the temporal warning, the system correctly generates the spatial warning at every frame. The system

TABLE II
EVENT-BASED AND FRAME-BASED SUCCESSFUL RATES AND FALSE WARNING RATE

Day / Night	Events	Events Hit	Events Miss	Events Hit rate	Frames	Frames base detect hit	Frames base detect miss	Micro hit rate
Day	53	49	4	92.45%	20766	17795	2971	85.69%
Night	49	45	4	91.83%	16601	13596	3005	81.89%
Day & Night	102	94	8	92.15%	37367	31391	5976	84.00%

starts to articulate the warning at the 73rd frame and stops at the 120th frame. On the other hand, the temporal warning is triggered at the 60th frame and fails to warn at the 90th and 110th frames. The fifth clip shows the no-street-light situation. In this case, the system will be affected by the head light of opposite-direction vehicles. We have unsatisfactory results since the detection of the lane boundaries is difficult in this case. However, when the real departure happened at the 885th frame, the system can still warn the driver correctly. The temporal warning is triggered at the 860th frame, but false positive is obtained at the 600th frame. The final clip shows a well-lighted situation. Our system successfully detects the lane boundaries and then triggers the warning signal. This effort is believed to be of good value and importance.

C. Event-Based Evaluation

In addition to evaluating the detection accuracy of the proposed algorithm on a single frame, we further validate this in terms of the lane departure events exhibited in the form of consecutive image frames. To extend our algorithm for detecting the departure events, we simply combine the results from N consecutive frames. In the warning mechanism for the departure events, the warning signal is triggered if and only if all the N consecutive frames are detected in dangerous situations. Here, the N is set as 5 in our experiment. We collect several videos in both daytime or nighttime under different conditions in a highway environment. After manually segmenting these videos, there are 53 and 49 lane departure events in daytime and nighttime, respectively. Furthermore, we classify these events into the following five categories for detailed analysis: 1) turning left fast; 2) turning left at slow speed; 3) turning right fast; 4) turning right at slow speed; and 5) go sharply. These 102 events are then used for experimental evaluation to validate our algorithm. The experimental results listed in Table II show the departure events in daytime, nighttime, and overall, respectively. Except for the case where the host vehicle turns right at slow speed in daytime and nighttime, this simple warning mechanism can achieve a high detection rate; moreover, the average event detection rates are 92.45% and 91.83% in daytime and nighttime, respectively. The improvement of the event-based detection algorithm can be made using some sophisticated strategies or probabilistic framework, e.g., Bayesian networks, to integrate the results from the proposed frame-based approach.

V. CONCLUSION

In this paper, we have presented a detailed software/hardware codesign of handheld real-time LDWS, which can easily be mounted on a real vehicle to dramatically improve driver safety. Such system with fruitful properties, such as compact size, low power consumption, and low cost, can widely be deployed to various popular consumer devices. In addition, this designed system makes lane departure detection more efficient and achieves high lane detection and warning detection rates. The proposed spatial and temporal lane departure warning mechanisms make us detect lane departure under a high vehicle departure speed and successfully avoid a false-alarm situation. Finally, six and 102 video clips for frame-based and event-based analyses are adopted to validate the effectiveness of our proposed system, respectively. However, this system will poorly perform if there is no sufficient illumination, such as that in the fifth video clip. In the near future, a more sophisticated algorithm, such as a tracking strategy, will be incorporated to solve this problem.

ACKNOWLEDGMENT

The authors would like to thank the reviewers for their detailed comments, which have improved the quality of this paper.

REFERENCES

[1] J. J. Segura-Jurez, D. Cuesta-Frau, L. Samblas-Pena, and M. Aboy, "A microcontroller-based portable electrocardiograph recorder," *IEEE Trans. Biomed. Eng.*, vol. 51, no. 9, pp. 1686–1690, Sep. 2004.
[2] A. Perea, T. Sundic, A. Pardo, R. Guitierrez-Osuna, and S. Marco, "A portable electronic nose based on embedded PC technology and GNU/Linux: Hardware, software and applications," *IEEE Sensors J.*, vol. 2, no. 3, pp. 235–246, Jun. 2002.
[3] F. Zuo and H. N. Peter, "Real-time embedded face recognition for smart home," *IEEE Trans. Consum. Electron.*, vol. 51, no. 1, pp. 183–190, Feb. 2004.
[4] J. Kaszubiak, M. Tornow, R. W. Kuhn, B. Michaelis, and C. Knoeppel, "Real-time vehicle and lane detection with embedded hardware," in *Proc. IEEE Intell. Vehicles Symp.*, Jun. 2005, pp. 619–624.
[5] C. R. Jung and C. R. Kelber, "A lane departure warning system based on a linear-parabolic lane model," in *Proc. IEEE Intell. Vehicles Symp.*, 2004, pp. 891–895.
[6] J. W. Lee, C. D. Kee, and U. K. Yi, "A new approach for lane departure identification," in *Proc. IEEE Intell. Vehicles Symp.*, 2003, pp. 100–105.
[7] P. L. Hsu, H.-Y. Cheng, B.-Y. Tsuei, and W.-J. Huang, "The adaptive lane-departure warning systems," in *Proc. SICE Annu. Conf.*, Aug. 2002, vol. 5, pp. 2867–2872.
[8] C. R. Jung and C. R. Kelber, "A lane departure warning system using lateral offset with uncalibrated camera," in *Proc. IEEE Conf. Intell. Transp. Syst.*, 2005, pp. 348–353.
[9] J. Kibbel, W. Justus, and K. Furstenberg, "Lane estimation and departure warning using multilayer laserscanner," in *Proc. IEEE Conf. Intell. Transp. Syst.*, 2005, pp. 777–781.
[10] P.-Y. Hsiao and C.-W. Yeh, "A portable real-time lane departure warning system based on embedded calculating techniques," in *Proc. IEEE Conf. Veh. Technol.*, May 2006, pp. 2982–2986.
[11] P. Jeong and S. Nedevschi, "Efficient and robust classification method using combined feature vector for lane detection," *IEEE Trans. Circuits Syst. Video Technol.*, vol. 15, no. 4, pp. 528–537, Apr. 2005.
[12] M. B. Ahmad and T.-S. Choi, "Local threshold and Boolean function based edge detection," *IEEE Trans. Consum. Electron.*, vol. 45, no. 3, pp. 674–679, Aug. 1999.
[13] S.-S. Huang, C.-J. Chen, P.-Y. Hsiao, and L.-C. Fu, "On-board vision system for lane recognition and front-vehicle detection to enhance driver's awareness," in *Proc. IEEE Int. Conf. Robot. Autom.*, 2004, vol. 3, pp. 2456–2461.
[14] A. Minagawa, Y. Kobayashi, N. Tagawa, and T. Tanaka, "Detection of vanishing point sequence with temporal fluctuation," *Syst. Comput. Jpn.*, vol. 34, no. 2, pp. 1–12, Feb. 2003.
[15] V. Cantoni, L. Lombardi, M. Porta, and N. Sicard, "Vanishing point detection: Representation analysis and new approaches," in *Proc. IEEE Int. Conf. Image Anal. Process.*, 2001, pp. 90–94.